

Orbital Kondo Effect in CrO_2 : A LSDA+DMFT Study

L. Craco, M. S. Laad and E. Müller-Hartmann

Institut für Theoretische Physik, Universität zu Köln, Zùlpicher Strasse, 50937 Köln, Germany

(February 1, 2008)

Motivated by a collection of experimental results indicating the strongly correlated nature of the ferromagnetic metallic state of CrO_2 , we present results based on a combination of the actual bandstructure [3] with dynamical mean-field theory (DMFT) for the multi-orbital case. In striking contrast with LSDA(+U) [3] and model many-body approaches [14], much better semiquantitative agreement with (i) recent photoemission results, (ii) domain of applicability of the half-metal concept, and (iii) thermodynamic and *dc* transport data, is obtained within a single picture. Our approach has broad applications for the detailed first principles investigation of other transition metal oxide-based half-metallic ferromagnets.

PACS numbers: 75.30.Mb, 74.80.-g, 71.55.Jv

A lot of attention has recently been focused on CrO_2 , widely used in magnetic recording, and with potential applications for spintronics [1,2]. In contrast to the CMR manganites, stoichiometric CrO_2 is already a ferromagnetic metal. Given the formal 4+ valence state of Cr , the two 3*d* electrons occupy t_{2g} orbitals. One would intuitively expect to form $S = 1$ spin on each site, and an antiferromagnetic Mott insulator. Why CrO_2 is a ferromagnetic metal instead, has been answered by Korotin *et al.* [3], who have carried out insightful (LDA + U) calculations for this material. Their main conclusions are: (i) The triple-degeneracy of the t_{2g} *d*-orbitals is lifted by tilting and rotation of the $Cr-O$ octahedra in the basic rutile structure, resulting in three bands with $xy, yz \pm zx$ character in the solid. The O 2*p* band(s) act, at least partially, as hole reservoirs resulting in Cr being mixed-valent (like Mn in doped manganites), explaining metallicity via self-doping in the negative charge-transfer situation realized in CrO_2 . (ii) an almost dispersionless majority spin band of predominantly *d* character at about 1 eV below E_F over a large region of the Brillouin zone. This corresponds to strongly localized xy orbitals completely occupied by one majority spin electron. But the *d* states (shown in Fig. 1) of predominantly $yz \pm zx$ character hybridize with the O 2*p* band and disperse, crossing E_F . The Hund's rule coupling between the localized d_{xy} spin and the spin density of the band $d_{yz \pm zx}$ electrons polarizes the latter, giving a ferromagnetic state via the double-exchange (DE) mechanism. Thus, both the metallicity and ferromagnetism are correlated well with each other.

Closer examination reveals that CrO_2 is a strongly correlated metal, implying that many-body correlation effects beyond the LDA [4] (or its variants) need to be considered. A number of experimental observations support such a view:

(1) Polarization dependent XAS measurements reveal substantial ligand orbital polarization. An exchange splitting energy of $\Delta_{ex-spl} \simeq 3.2$ eV was deduced [5], implying substantial correlation effects, while LSDA cal-

culations yield $\Delta_{ex-spl} \simeq 1.8$ eV!

(2) The resistivity has a characteristic correlated Fermi liquid (FL) form [6]: $\rho(T) = \rho_0 + AT^2 + BT^{7/2}$ [7], and, in fact, CrO_2 is a "bad metal" at high- T , with $\rho_{dc}(T > T_c^{FM} = 390K)$ exceeding the Mott limit [8]. The Woods-Saxon ratio A/γ^2 is close to that expected for heavy-fermion metals [8], implying substantial correlation effects in the Cr *d*-band.

(3) Optical conductivity studies reveal a Drude part at low energies, followed by a broad bump around 0.8 eV and high-energy features centered around 3 eV. LDA+U predicts only the small Drude part correctly [9]. In addition, noticeable spectral weight transfer (SWT) from high to low energy is found as T is reduced [9]. This SWT scales with magnetization, $M(T)$, as in the CMR materials [10], showing clearly the correlated nature of the metallic state (the SWT is a *dynamical* many body correlation effect, and cannot be accessed by LSDA+U).

(4) Recent measurements show that the integrated photoemission (PES) lineshape is characterized by a low-energy quasicohherent feature along with an incoherent [11,12] broad feature at lower energies. This satellite feature observed in PES is a signal for the importance of dynamical, many-body correlation effects beyond LDA+U.

(5) Finally, recent optical [10] and tunnelling measurements [13] show half-metallic character only close to (about $\simeq 0.5$ eV around) E_F . Direct comparison with LSDA+U shows that these calculations would yield half-metallicity up to 1.5 eV. It is not easy to cure this within LSDA+U. One could, of course, refer to LSDA results, where the minority-spin band does have a threshold around 0.6 eV, but LSDA gives results directly in conflict with (1)-(4).

The emergence of a correlated FL scale required to understand the above features is out of reach of LSDA or pure DE models, because these are observed well below T_c^{FM} , and are thus related to additional scattering mechanisms in a half-metallic situation. We argued previously [14] that the above effects could be understood

by invoking the important role of local, dynamical orbital correlations in the t_{2g} sector. However [14], a model (gaussian) density of states was used there, limiting direct comparison to experimental results. To do this, one has to extend a model-based approach to include real bandstructure features via the LDA+DMFT method. We choose LDA+DMFT because although approximations like LSDA+U do generate the correct ordered, *insulating* state(s), they fail to describe the correlated paramagnetic states, or the Mott transition accompanied by dynamical SWT. As discussed in detail [15], very good agreement with experiment is achievable within LDA+DMFT. In practice, this is a highly non-trivial task, and very computationally expensive. Here, we describe CrO_2 within this “first-principles bandstructure” for correlated metals. The results are found to be in very good semiquantitative agreement with experiments probing both the occupied parts of the one-particle DOS ($\rho(\omega)$) as well as with thermodynamic and dc transport data cited above.

An understanding of features mentioned above should go hand-in-hand with the basic electronic structure. Our starting point is the LSDA+U work of Korotin *et al.* [3], which yields the one-particle bandstructure of CrO_2 (notice that the Hartree-Fock shift is already incorporated in LSDA+U). In Fig. 1, we show the partial t_{2g} DOS for the half-metallic situation realized in CrO_2 . In the real material, only the t_{2g} states of Cr hybridized with O -2p states are important, and so we neglect the higher energy e_g bands. Following [3], we suppose the O -2p states to introduce a small number of holes into the $d_{yz\pm zx}$ bands. In fact, $\int_{-1.5}^{1.3} \rho_{\uparrow}^{t_{2g}}(\omega) d\omega = 1.82 < 2$. Given that the O -2p spectral density is small compared to $\rho_{\uparrow}^{t_{2g}}(\omega)$, we keep only the t_{2g} bands in what follows. With the LSDA bandstructure, the one-particle part of the Hamiltonian is:

$$H_0 = \sum_{\mathbf{k}, \alpha, \beta} \epsilon_{\alpha\beta}(\mathbf{k}) c_{\mathbf{k}\alpha\sigma}^{\dagger} c_{\mathbf{k}\beta\sigma} \quad (1)$$

with $\rho_{\uparrow}^{t_{2g}}(\omega) = \sum_{\mathbf{k}, \alpha, \beta} \delta(\omega - \epsilon_{\alpha\beta}(\mathbf{k}))$ and $\alpha, \beta = xy, yz \pm zx$. To avoid double counting of Coulomb interaction contributions already contained in H_{LDA} , a term H_{LDA}^U is subtracted from H_0 . Following [15], the final result is,

$$H_0 = \sum_{\mathbf{k}, \alpha, \beta} \epsilon_{\alpha\beta}(\mathbf{k}) c_{\mathbf{k}\alpha\sigma}^{\dagger} c_{\mathbf{k}\beta\sigma} + \sum_{i\alpha\sigma} \epsilon_{i\alpha\sigma}^0 n_{i\alpha\sigma}, \quad (2)$$

where $\epsilon_{i\alpha\sigma}^0 = \epsilon_{i\alpha\sigma} - U(n_{\alpha\sigma} - 1/2) + (1/2)J_H(n_{\alpha\sigma} - 1)$, and U and J_H are defined below in H .

The full many body Hamiltonian for CrO_2 is:

$$H = H_0 + \frac{1}{2} \sum_{i\alpha\beta\sigma\sigma'} U_{\alpha\beta}^{\sigma\sigma'} n_{i\alpha\sigma} n_{i\beta\sigma'} - \frac{1}{2} \sum_{i\alpha\beta\sigma\sigma'} J_H \mathbf{S}_{i\alpha} \cdot \mathbf{S}_{i\beta}. \quad (3)$$

To make progress, we notice that LSDA+U pushes the minority spin t_{2g} bands to high energy $\omega > 2\text{eV}$. To

begin with, we focus on the majority-spin t_{2g} sector. A valid choice of parameters to describe this situation is given by the intra-orbital $U = 5\text{ eV}$, and the Hund’s rule coupling $J_H = 1\text{ eV}$, close to the LSDA deduced values, along with the inter-orbital local interaction, $U' = U - 2J_H$, for t_{2g} orbitals. Notice that U', J_H couple the three $xy, yz \pm zx$ bands, requiring an extension to treat multi-orbital effects.

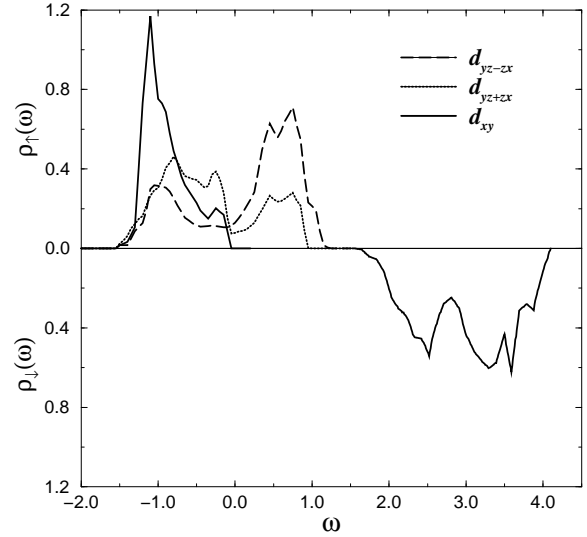


FIG. 1. t_{2g} LSDA+U density of states per formula unit for both spin channels obtained from [3], Figs. 3 (spin-down) and 4 (spin-up).

We solve this multiband hamiltonian in $d = \infty$ using the iterated perturbation theory (IPT), suitably generalized for the multi-orbital case. Notice that CrO_2 falls into the class of TM oxides with well-separated t_{2g} and e_g bands [3]. Moreover, $G_{\alpha\beta\sigma\sigma'}(\omega) = \delta_{\alpha\beta}\delta_{\sigma\sigma'}G_{\alpha\sigma}(\omega)$ and $\Sigma_{\alpha\beta\sigma\sigma'}(\omega) = \delta_{\alpha\beta}\delta_{\sigma\sigma'}\Sigma_{\alpha\sigma}(\omega)$.

In the t_{2g} sub-basis, a DMFT solution involves (i) replacing the lattice model by a self-consistently embedded multi-orbital, asymmetric Anderson impurity model, (ii) and a self-consistency condition which requires the local impurity Green function to be equal to the local GF for the lattice, given by

$$G_{\alpha}(\omega) = \frac{1}{V_B} \int d^3k \left[\frac{1}{(\omega + \mu)1 - H_{LSDA}^0(\mathbf{k}) - \Sigma(\omega)} \right]_{\alpha}. \quad (4)$$

Using the locality of $\Sigma_{\alpha\beta}$ in $d = \infty$, we have $G_{\alpha}(\omega) = G_{\alpha}^0(\omega - \Sigma_{\alpha}(\omega))$ using the Hilbert transform of the LSDA DOS. In contrast to [15], the inter-orbital coupling scatters electrons between the $xy, yz \pm zx$ bands, so only the total number, $n_{d_{t_{2g}}} = \sum_{\alpha} n_{d_{t_{2g}}, \alpha}$ is conserved in a manner consistent with Luttinger’s theorem. Further, in CrO_2 , due to a highly asymmetric LDA DOS (Fig. 1), we expect the final spectral function to reflect the interplay of the complicated bandstructure and inter-orbital

correlations.

The calculation follows the philosophy of the IPT for the one-band Hubbard model, but the self-energies and propagators are matrices in the orbital indices [16]. Leaving details for a longer paper, we present here the final equations. The local propagators are given by,

$$G_\alpha(\omega) = \frac{1}{N} \sum_{\mathbf{k}} \frac{1}{\omega - \Sigma_\alpha(\omega) - \epsilon_{\mathbf{k}\alpha}}, \quad (5)$$

where $\alpha = xy, yz \pm zx$. The local self-energies are computed from a generalized IPT formalism that takes into account the Luttinger theorem constraint off half-filling [15] (generalized Friedel sum rule). Explicitly,

$$\Sigma_\alpha(\omega) = \frac{A_\alpha[\Sigma_{\alpha\alpha}^{(2)}(\omega) + \Sigma_{\alpha\beta}^{(2)}(\omega) + \Sigma_{\alpha\gamma}^{(2)}(\omega)]}{1 - B_\alpha[\Sigma_{\alpha\alpha}^{(2)}(\omega) + \Sigma_{\alpha\beta}^{(2)}(\omega) + \Sigma_{\alpha\gamma}^{(2)}(\omega)]} \quad (6)$$

where, for example, $(\alpha \neq \beta \neq \gamma)$

$$\Sigma_{\alpha\beta}^{(2)}(i\omega) = \left(\frac{U_{\alpha\beta}}{\beta}\right)^2 \sum_{n,m} G_\alpha^0(i\omega_n) G_\beta^0(i\omega_m) G_\beta^0(i\omega_n + i\omega_m - i\omega) \quad (7)$$

and $G_\alpha^0(\omega) = [\omega + \mu_\alpha - \Delta_\alpha(\omega)]^{-1}$. In Eqn. (6), $A_\alpha = \frac{n_\alpha(1-2n_\alpha) + D_{\alpha\beta}[n]}{n_\alpha^0(1-n_\alpha^0)}$ and $B_\alpha = \frac{(1-2n_\alpha)U_{\alpha\beta} + \epsilon_\alpha - \mu_\alpha}{2U_{\alpha\beta}^2 n_\alpha^0(1-n_\alpha^0)}$.

Here, n_α and n_α^0 are particle numbers determined from G_α and G_α^0 respectively, and $D_{\alpha\beta}[n] = \langle n_{\alpha\sigma} n_{\beta\sigma'} \rangle$ is calculated using $\langle n_{\alpha\sigma} n_{\beta\sigma'} \rangle = \langle n_{\alpha\sigma} \rangle \langle n_{\beta\sigma'} \rangle - \frac{1}{U'\pi} \int_{-\infty}^{+\infty} f(\omega) [\Sigma_\alpha(\omega) G_\alpha(\omega)] d\omega$. The last identity follows directly from the equations of motion for $G_\alpha(\omega)$.

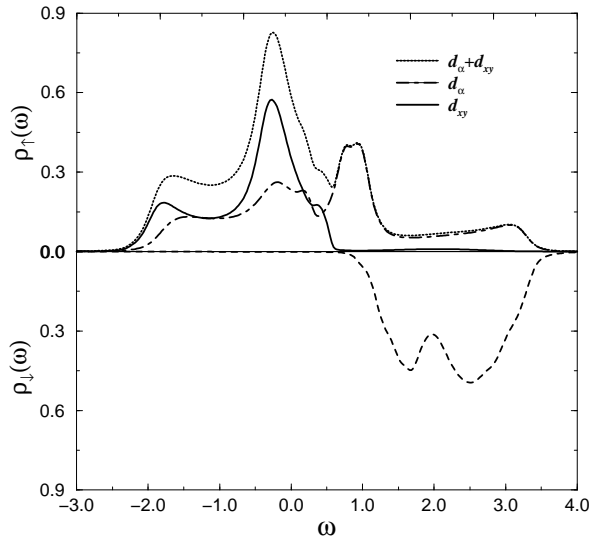


FIG. 2. LSDA+DMFT partial and total density of states for the Cr t_{2g} orbitals for $U' = 3.0$ eV.

We now present our results. In Fig. 2, we show the renormalized, total spectral function (sum of the partial

t_{2g} DOS) of CrO_2 for $T = 0$. Notice the high-energy “Hubbard bands” appearing as manifestations of dynamical effects of strong orbital correlations in the t_{2g} sector. As is also clear, the Luttinger theorem is obeyed to a very good accuracy. Additionally, the self-energies show characteristic correlated Fermi liquid behavior. Based on these results, we interpret the low energy quasicohherent features as arising from collective *orbital* Kondo screening of t_{2g} orbital moments in the fully spin polarized half-metal.

We emphasize the quantitative differences between the results of this work with an earlier one [14], where an idealized (gaussian) unperturbed DOS was used; no low-energy (LSDA related) pseudogap-like feature was visible there. Further, the d_{xy} band was replaced there by a dispersionless, local level playing the role of polarizing the $yz \pm zx$ bands via strong J_H , making it impossible to access changes resulting from the interplay of the realistic bandstructure and strong orbital correlations. These differences are especially important when one attempts to describe spectroscopy results quantitatively (see below).

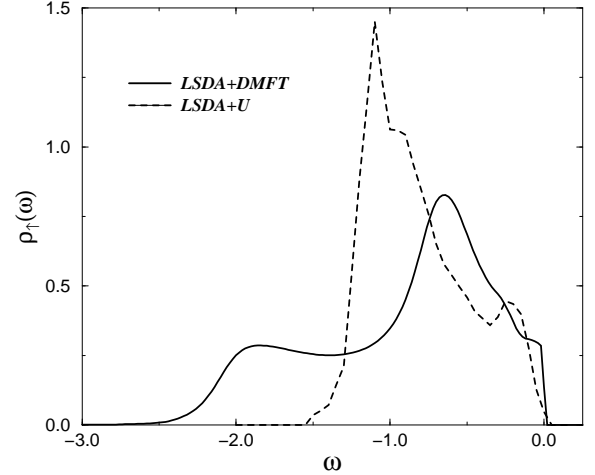


FIG. 3. The integrated photoemission lineshapes for the spin-up channel within LSDA+DMFT for $U' = 3.0$ eV (solid line) and LSDA+U (dashed line).

In Fig. 3, we show the integrated PES lineshape for low T , obtained directly from $I_{PES}(\omega) = f_F(\omega - E_F) \rho_{\uparrow}^{t_{2g}}(\omega)$. Quite satisfyingly, the quasicohherent spectral weight at μ is larger than what was reported in earlier experimental work [11], and in quite good agreement with results obtained recently from thin films [12]. In particular, it is gratifying to see good quantitative agreement between theory and experiment in the region $-1.2 < \omega \leq E_F$. Specifically, the small, but clear dip seen in the LSDA+U DOS is absent in LSDA+DMFT, in agreement with the thin film results. At higher binding energy, we do not expect quantitative agreement because both $O-2p$ and e_g

bands of Cr begin to contribute, and also because the minority spin t_{2g} band leads to a breakdown of our approach, which neglected the minority-spin sector. Consequently, further work is needed to make comparison with the recent tunnelling and optical measurements [9,13], since these measurements probe the minority spin band at higher energies. Optical measurements reveal that the almost complete spin polarization near E_F is reduced at higher energy $\omega \geq 0.5$ eV.

To this end, we extend the above calculation to include the minority-spin t_{2g} bands, which (see Fig. 1) are pushed to high energy $\omega > 2$ eV by LSDA+U. Inter-orbital correlations between the $t_{2g} \uparrow, \downarrow$ bands are accounted for in a way similar to that described above for the majority-spin sector. However, a larger $U_{\uparrow\downarrow} = U' + 2J_H$ is now required for the calculation of the minority spin DOS, $\rho_{\downarrow}^{t_{2g}}(\omega)$, along with a Hartree shift of $-J_H m$ (where m is the magnetization per site) for the \downarrow -spin sector. The interaction-corrected minority spin DOS (lower panel of Fig. 2) shows interesting features. First, $U_{\uparrow\downarrow}$ broadens out the sharp LSDA features, and more importantly, transfers dynamical spectral weight from high- to lower energy $\omega \simeq 0.7$ eV. As a result, above 0.7 eV, the spin polarization decreases continuously from saturation, in nice agreement with indications from optical and tunnelling measurements [9,13]. Notice that LSDA+U would predict complete half-metallicity up to a much higher energy $\simeq 1.5$ eV. This represents strong evidence for the importance of treating dynamical SWT correctly, an effect missed by LSDA+U, but treated adequately by LSDA+DMFT. In fact, in our view, optical and tunnelling results provide a direct confirmation of the importance of dynamical correlation effects. Indeed, one could argue that the near similarity of the LSDA- and LSDA+DMFT spectral functions for t_{2g}^{\uparrow} sector for $-0.7 \leq \omega \leq 0.2$ eV is a sign of the adequacy of LSDA+U. As discussed above, however, consistency with optics and tunnelling results as well is only achieved within LSDA+DMFT.

The results obtained above are also consistent with the low- T thermodynamic and dc resistivity of CrO_2 . Indeed, from the computed self-energy, we estimate a moderate quasiparticle renormalization, Z . From the fact that $\text{Im}\Sigma_{yz\pm zx}(\omega) \simeq -b\omega^2$, we infer that the low- T dc resistivity should follow $\rho_{dc}(T) = \rho_0 + AT^2$. In fact, using $A = (m^*/ne^2)(\partial^2\Sigma(\omega)/\partial\omega^2)_{\omega=E_F}$ from $\text{Im}\Sigma_{yz\pm zx}(\omega)$, we estimate the Woods-Saxon ratio, $A/\gamma^2 \simeq 3.5 \cdot 10^{-5}$, close to the value found experimentally [8].

To conclude, we have extended the LSDA+U calculation [3] to explicitly include the dynamical correlation effects arising from local electronic correlations in the t_{2g} sector in the multi-orbital system CrO_2 . Puzzling signatures of strong correlations in the half-metallic state are understood as manifestations of collective orbital Kondo effect in the t_{2g} sector, originating from a non-trivial interplay between the realistic hopping in the

rutile structure and inter-orbital (t_{2g}) correlations. Much better quantitative agreement with PES is obtained with LSDA+DMFT than with LSDA or LSDA+U, showing clearly the importance of dynamical correlation effects. Further, our results are also in semiquantitative agreement with thermodynamic and dc transport measurements. Essentially similar techniques can also be used fruitfully for other transition metal oxide-based ferromagnets currently of great interest [17].

Work carried out under the auspices of the Sonderforschungsbereich 608 of the Deutsche Forschungsgemeinschaft.

-
- [1] J. M. D. Coey *et al.*, Adv. Phys. **48**, 167 (1999).
 - [2] H. Ohno, Science **281**, 951 (1998). Also, see B. Martinez *et al.*, J. Appl. Phys. **87**, 6019 (2000).
 - [3] M. Korotin *et al.*, Phys. Rev. Lett. **80**, 4305 (1998).
 - [4] I. Mazin, D. J. Singh, and C. Ambrosch-Draxl, Phys. Rev. B **59**, 411 (1999).
 - [5] G. Stagarescu *et al.*, cond-mat/9910346, to be published in Phys. Rev. B.
 - [6] L. Ranno, A. Barry, and J. M. D. Coey, J. Appl. Phys. **81**, (8), 5774 (1997).
 - [7] V. Yu. Irkhin and M. Katsnelson, Phys. Usp. **37**, 659 (1994).
 - [8] K. Suzuki and P. Tedrow, Phys. Rev. B **58**, 17, 11597 (1998).
 - [9] E. Singley, C. Weber, D. Basov, A. Barry, and J. M. D. Coey, Phys. Rev. B **60**, 4126 (1999).
 - [10] R. Yamamoto, Y. Moritomo, and A. Nakamura, Phys. Rev. B **61**, R5062 (2000).
 - [11] K. Kämper, W. Schmitt, G. Güntherodt, R. Gambino, and R. Ruf, Phys. Rev. Lett. **59**, 2788 (1987).
 - [12] Recent results by D. J. Huang and H. Tjeng (unpublished) do show a quasicohherent low-energy feature with almost 100 percent spin-polarization, in disagreement with earlier work.
 - [13] Y. Ji *et al.*, Phys. Rev. Lett. **86**, 5585 (2001).
 - [14] M. S. Laad, L. Craco, and E. Müller-Hartmann, Phys. Rev. B **64**, 214421 (2001).
 - [15] see A. Georges, G. Kotliar, M. Rozenberg, and M. Caffarel, Revs. Mod. Phys. **68**, 13 (1996). For recent developments including LDA bandstructure, see K. Held *et al.*, cond-mat/0112079.
 - [16] S. Y. Savrasov, G. Kotliar, and E. Abrahams, Nature **410**, 793 (2001). See also, A. I. Lichtenstein *et al.*, Phys. Rev. B **57**, 6884 (1998); V. Anisimov *et al.*, J. Phys. Condens. Matter, **9**, 7359 (1997).
 - [17] J.-H. Park *et al.*, Nature **392**, 794 (1998).